NANO LETTERS

Letter

pubs.acs.org/NanoLett

The Race of Nanowires: Morphological Instabilities and a Control Strategy

Sangwoo Shin,[†,§] Talal T. Al-Housseiny,[‡,†,§] Beom Seok Kim,[∥] Hyung Hee Cho,*[,∥] and Howard A. Stone*[,†]

[†]Department of Mechanical and Aerospace Engineering and [‡]Department of Chemical and Biological Engineering, Princeton University, Princeton, New Jersey 08544, United States

[∥]Department of Mechanical Engineering, Yonsei University, Seoul 120-749, Korea

Supporting Information

ABSTRACT: The incomplete growth of nanowires that are synthesized by template-assisted electrodeposition presents a major challenge for nanowire-based devices targeting energy and electronic applications. In template-assisted electrodeposition, the growth of nanowires in the pores of the template is complex and unstable. Here we show theoretically and experimentally that the dynamics of this process is diffusion-limited, which results in a morphological instability driven by a race among nanowires. Moreover, we use our findings to devise a method to control the growth instability. By introducing a temperature gradient across the porous template, we manipulate ion diffusion in the pores, so that we can reduce the growth instability. This strategy significantly increases the length of nanowires. In addition to shedding light on a key nanotechnology, our results may provide fundamental insights into a variety of interfacial growth processes in materials science such as crystal growth and tissue growth in scaffolds.

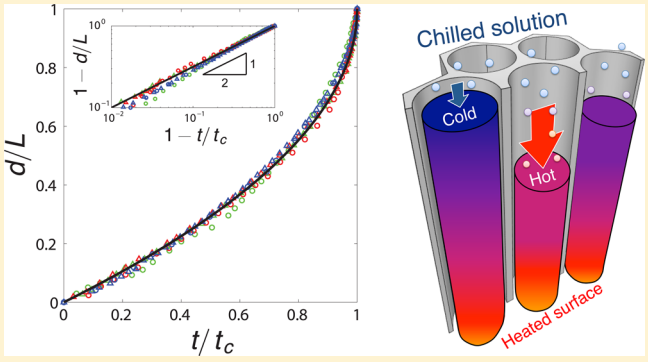

KEYWORDS: *Nanowires, template-assisted electrodeposition, morphological instability, diffusion, temperature gradient*

Exploiting nanowires as a material for future electronics[1−3] and energy[4−6] applications has been one of the main topics in nanotechnology. The synthesis of nanowires for such widespread applications requires scalability, density, reproducibility and cost effectiveness. In this regard, template-assisted electrodeposition offers distinct advantages[7,8] for synthesizing nanowires. This method uses a physical template, which is a porous structure, to grow the desired nanowires in its long and narrow pores by electrochemically depositing the ions that are present in a surrounding solution. In general, templates with closely packed pores, such as anodic aluminum oxide (AAO) membranes, allow the production of dense arrays of nanowires. Furthermore, the porous template provides mechanical robustness and serves as an electrical insulator between the tightly spaced nanowires.

In template-assisted electrodeposition, a nanowire must span the entire length of a given pore in order to connect both ends and, hence, conduct current.[9] However, fully grown nanowires constitute only a tiny fraction of the total number of nanowires, which presents a major challenge.[10,11] This fraction is normally far less than 1%.[12] As shown in Figure 1, parts a and b, once a fast-growing nanowire reaches the top of the pore, it protrudes out of the template and undergoes an unbounded growth.[12,13] Eventually, nearby pores are blocked, which prematurely terminates the growth of adjacent nanowires. The end result consists of a long nanowire with a mushroom-like overdeposit surrounded by a large number of short immature nanowires.

These unfavorable nanowire growth conditions, which are commonly observed,[10,12,14−17] were initially attributed to electric effects.[14,15] Then, it was suggested that the diffusion of ions in the slender pores could also be governing the unstable growth process.[10,17,18] The fundamental mechanism of this morphological growth instability of nanowires remains unclear owing to the complexity of electrodeposition and its sensitivity to many factors such as temperature,[19] solution conductivity,[20] ion concentration,[21] pH,[21] quality of the template,[10] etc. Nevertheless, there is great interest in controlling the growth instability and facilitating the complete growth of nanowires. To this end, several methods have been proposed such as lowering the overall temperature of the system[10,17] and using pulsed electrodeposition.[16,17]

Here, we describe the growth dynamics in template-assisted electrodeposition. Under diffusion-limited conditions, the growth of nanowires follows a universal behavior, which is independent of system parameters. Our results expose the underlying mechanism for the morphological instability. To test

Received: April 9, 2014
Revised: June 15, 2014
Published: June 27, 2014

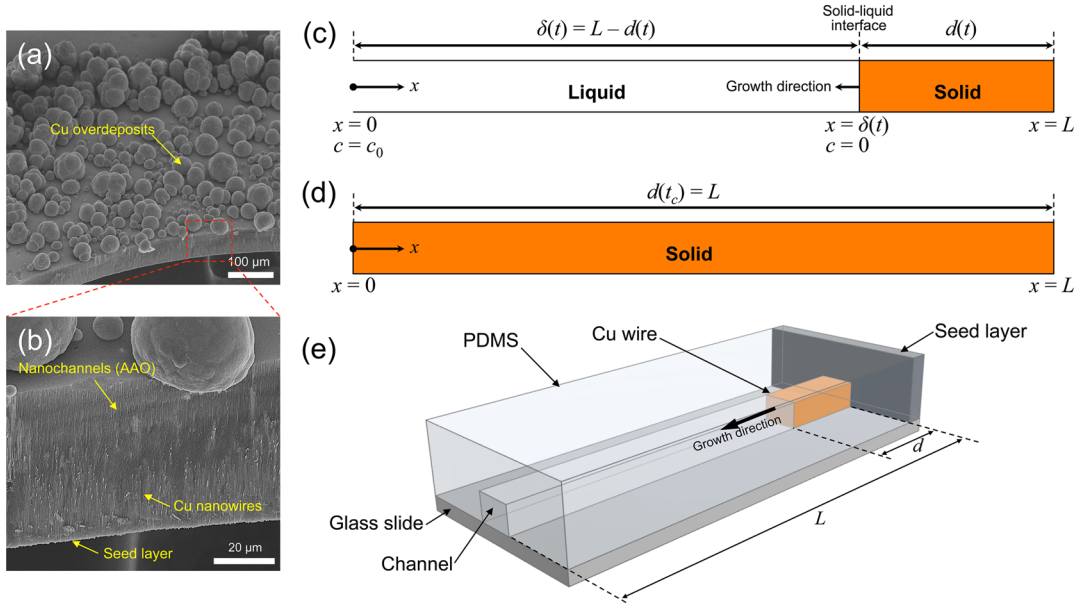

Figure 1. Nanowire growth instabilities in template-assisted electrodeposition. (a) Scanning electron microscope (SEM) image of copper nanowires mushrooming out of the pores of AAO membranes (adapted with permission from ref 12). The overdeposits accumulating on the membrane block adjacent nanopores. (b) Close-up view of the cross-section of the template in (a) to highlight the nonuniform and unstable growth of nanowires. (c, d) Schematics of the growth process of a single nanowire in a slender pore. (d) When the solid−liquid interface reaches the end of the pore, $x = 0$, then $t = t_c$. (e) Schematic of our model experiment, which allows us to monitor the real-time growth of a single wire in a microchannel.

the dynamics in a well-controlled environment, we conduct microscale experiments that mimic the observed nanoscale phenomenon. On the basis of our findings, we seek to effectively control the growth instability in template-assisted electrodeposition. In the presence of an applied temperature gradient, we find that the penetration of nanowires into the pores and the average nanowire length is significantly improved.

To examine the growth dynamics of the nanowires in the porous template, we focus on a single liquid-filled pore, into which metal ions diffuse from the surrounding electrolyte whose bulk concentration is c_0. In the case of AAO membranes for example, a pore is of the order of 100 nm in diameter and 10 μm in length.[17,19] This high aspect ratio indicates that the concentration of ions $c(x,t)$ in the pore of length L can be described by a one-dimensional diffusion process

$$\frac{\partial c}{\partial t} = D\frac{\partial^2 c}{\partial x^2}, \quad x \in [0, \delta(t)], \quad t \in [0, t_c] \tag{1}$$

where x is the position away from the pore entrance as displayed in Figure 1c, t is the time since the growth process has started, and D is the diffusion coefficient. At the solid−liquid interface denoted by $x = \delta(t)$, the reduced metal ions accumulate and form a growing nanowire of length $d(t)$. At the end of the growth process, that is, at a critical time $t = t_c$, the nanowire reaches the end of the pore such that $d(t_c) = L$, as illustrated in Figure 1d.

The nanowire growth into the liquid-filled portion of the pore $\delta(t)$ is a two-phase free-boundary problem, which is a variant of the classical Stefan problem.[22,23] In the limiting case where the diffusion of ions is much slower than the interfacial growth, the dynamics can be assumed quasi-steady similar to the Arnold cell setup.[24] Here we consider the full unsteady problem. The growth speed is proportional to the flux of ions toward the solid−liquid interface, which yields the boundary condition[25]

$$-D\left.\frac{\partial c}{\partial x}\right|_{x=\delta(t)} = -\frac{A\rho}{M_W}\frac{\mathrm{d}\delta}{\mathrm{d}t} \tag{2}$$

where ρ and M_W are the density and the molecular weight of the nanowire, respectively. The parameter A is a measure of the efficiency of the electrochemical conversion.

The driving force for the diffusion of ions across the pore is the overall concentration gradient $\sim c_0/\delta(t)$, which sets the growth speed of the interface (eq 2). Therefore, as $\delta(t)$ decreases in time (Figure 1c and d), the concentration gradient and the growth speed increase and blow up at $t = t_c$ since $\delta(t_c) = 0$. This finite-time singularity inspires us to work in reverse time $t_c - t$. Hence, we find that the solution to this finite-pore diffusion problem, and so the growth of the nanowires, is governed by self-similar dynamics,

$$\frac{c(x,t)}{c_0} = 1 - \frac{\mathrm{erfi}(\beta\eta)}{\mathrm{erfi}(\beta)}, \quad \eta = \frac{x}{\delta(t)}, \qquad \delta(t) = 2\beta\sqrt{D(t_c - t)} \tag{3}$$

where η is the similarity variable and erfi is the imaginary error function. The dimensionless prefactor β is obtained by substituting the concentration profile (eq 3) into the interfacial condition (eq 2), so that[26]

$$\beta e^{-\beta^2}\mathrm{erfi}(\beta) = \frac{M_W c_0}{\sqrt{\pi}A\rho} \tag{4}$$

The dynamics of the diffusion process in the nanopore is presented in Figure 2, where different values of β are considered; β is also given as a function of $M_W c_0/A\rho$ (see Figure 2b). Observe that our definition for the diffusive length $\delta(t)$ in eq 3 requires that $t_c = (L/2\beta\sqrt{D})^2$ based on the initial conditions.

We now use the previous results toward our main objective, which is determining the growth dynamics of the nanowire. Since $d(t) + \delta(t) = L$, we obtain

dx.doi.org/10.1021/nl501324t | Nano Lett. 2014, 14, 4395−4399

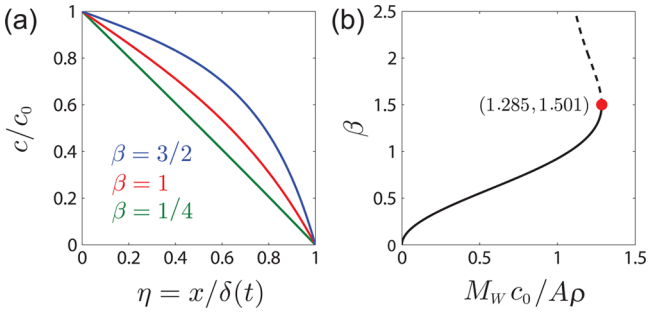

Figure 2. (a) Concentration profile of diffusing ions, given by eq 3, for various values of β. (b) Transcendental equation given in eq 4 yields the prefactor β as a function of $M_W c_0/A\rho$. The fixed point (red dot) delineates the boundary between physical (——) and unphysical (– – –) solutions.

$$\frac{d(t)}{L} = 1 - \sqrt{1 - \frac{t}{t_c}} \tag{5}$$

Scaling the nanowire length $d(t)$ by L and time by t_c , it becomes clear that the dynamics in eq 5 is independent of any parameters and, thus, follows a universal behavior.

To verify our theoretical findings, we realize a controlled model experiment that mimics the nanowire growth conditions (see Supporting Information). A schematic of the microscale diffusion-limited experimental setup is displayed in Figure 1e. We track the growth of an individual Cu wire in a 100 μm × 100 μm slender channel, which is made in transparent polydimethylsiloxane (PDMS) using standard soft lithography techniques. By changing the length of the channel and the bulk concentration of the $CuSO_4$ electrolyte, we vary both L and t_c. As shown in Figure 3, the growth dynamics for different

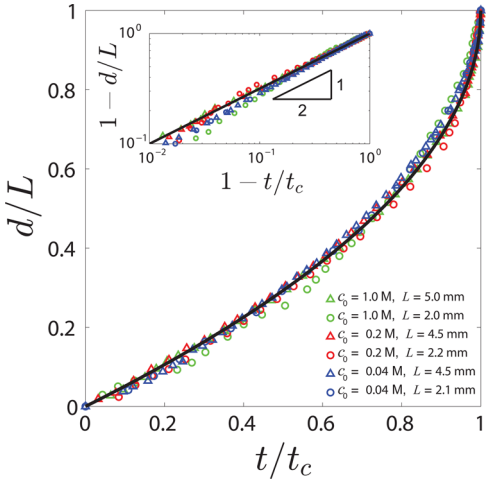

Figure 3. Growth dynamics of Cu wires grown in slender microchannels. The symbols represent experimental results whereas the solid curve is a plot of eq 5, which has no fitting parameters. The inset features the 1/2 diffusive scaling through a log–log plot. The error bars are of the size of the symbols.

experimental conditions collapse onto a universal curve, which reflects the excellent agreement with our predictions (see Supporting Information).

The universal dynamics we identify exposes the mechanism of the growth instability. According to eq 5, the growth continuously accelerates in time especially as the nanowire gets closer to the end of the pore; see Figure 3. Any perturbation such as irregularities in the pores or the seed layer[17] and nonconcurrent pore nucleation[10,17,21] can be amplified tremendously with time. Let us examine, for instance, the effect of a small nonuniformity in pore length. Consider one pore of length L and a second one that is εL longer, where the perturbation $\varepsilon \ll 1$. A simple calculation shows that, at the time when the nanowire in the shorter pore becomes fully grown with a length L, the nanowire in the longer pore is $\simeq (2\varepsilon)^{1/2}L$ shorter. For example, a 5% longer pore yields a 32% shorter nanowire. Essentially, the nanowire in the shorter pore outraces the second nanowire to the top of the template. In such a case, there would be enough time for the fully grown nanowire to mushroom out, blocking the nearby pores as shown in Figure 1a.

The dynamics that we have just identified can also explain why reducing the overall temperature can promote more uniform nanowires,[10,17] where in the previous works the exact mechanism was unclear. When the temperature is decreased, the growth rate is significantly reduced, whereas the initial perturbation (defects and/or nucleation) remains almost unchanged.[17] For example, suppose that there are two nanowires of the same length. However, one nanowire is nucleated after time t_n has passed since the nucleation of the other nanowire. Then, the length difference of the two nanowires at the time one reaches the end of the pore, i.e., $t = t_c$, is $(t_n/t_c)^{1/2}$. Thus, the final length difference is determined by t_c and t_n. Reducing the overall temperature significantly increases t_c while t_n remains almost the same, which leads to a smaller length difference. Therefore, we expect and have shown that reducing temperature reduces the length difference of the nanowires, thereby increasing the overall length of the nanowires.

Now that we understand the mechanism of the nanowire growth instability, we have an opportunity to put forward an effective method to control the instability. The diffusive nature of the instability drives the accelerating growth of nanowires. Thus, we expect that a spatial control of diffusion presents a promising strategy to enhance the length and the uniformity of nanowires.

Applying a temperature gradient across the porous template leads to spatial variations in the diffusion coefficient. This approach is realized by setting the seed layer at a higher temperature than that of the electrolyte. A schematic of our control scheme is illustrated in Figure 4a. Along a given pore, the temperature gradually decreases from the seed layer to the electrolyte solution. Consequently, since diffusion is slower at lower temperatures, the temperature gradient promotes the growth of lagging nanowires over leading ones. In other words, the effect of the applied gradient counteracts or stabilizes the accelerating growth dynamics, induced by the shrinkage of the diffusion region $\delta(t)$. In previous studies,[27−29] the use of gradients has been proven successful in controlling interfacial instabilities.

We perform template-assisted electrodeposition experiments in the presence of a temperature gradient (see Supporting Information). We grow bismuth nanowires, which are known for their good thermoelectric properties at the nanoscale,[30] in porous AAO membranes. While the electrolytic solution is maintained at 10.1 °C, we vary the temperature of the seed layer, so that the magnitude of the temperature gradient is varied. Once the nanowires are grown to maturity, which is when pores are blocked by overdeposits similar to Figure 1a, we

dx.doi.org/10.1021/nl501324t | Nano Lett. 2014, 14, 4395−4399

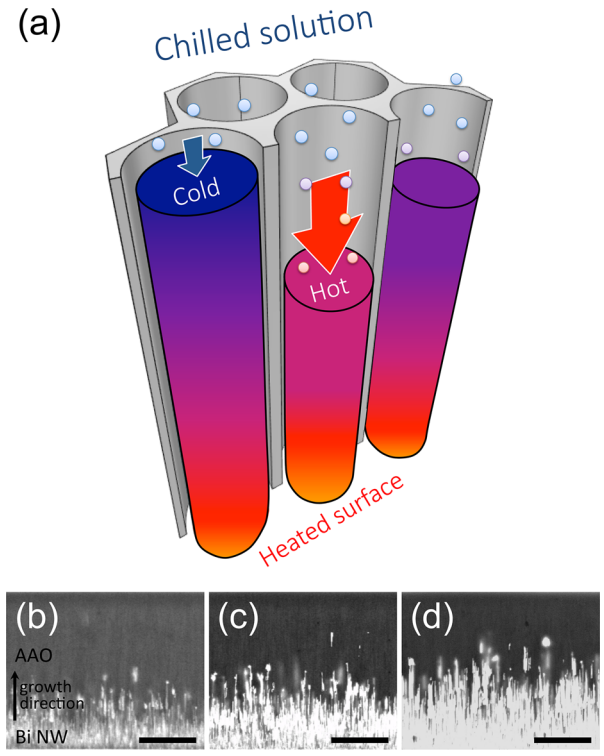

Figure 4. Controlling the nanowire growth instability. (a) Schematic of our control protocol, which applies a temperature gradient across the porous template. (b–d) Backscattered SEM images of bismuth nanowires grown in AAO membranes. The seed layer temperature is set at (b) 10.1, (c) 17.1, and (d) 28.8 °C. The electrolyte is maintained at 10.1 °C in all cases. Hence, the temperature gradient increases from left to right. The average nanowire length to pore length is estimated at (b) 25.3% (control experiment), (c) 32.7%, and (d) 44.9%. All the scale bars are 20 μm.

cleave the porous membrane to get a cross-sectional view of the encased nanowires. Consistent with our original expectation, significantly longer nanowires are produced in the presence of a small temperature gradient, as shown in Figure 4b–d. In addition, we find that the ratio of nanowire length to pore length increases with the applied gradient and reaches almost 45% of the total. Our experimental results demonstrate the stabilizing effect and improvement opportunities offered by our control strategy.

In summary, template-assisted electrodeposition is hindered by a morphological instability, which limits the growth of nanowires in the pores. Overdeposits accumulating on the template block the pores, not allowing metal ions to penetrate. We theoretically and experimentally characterized the growth dynamics of electrodeposited nanowires in porous structures. The growth dynamics we identified reveal the mechanism of the instability. As nanowires grow, the diffusion of electrolytes into pores continuously accelerates, which drives the growth instability. On the basis of our findings, we implemented a strategy to control the instability. By introducing a small temperature gradient across the porous template, we can enhance the growth of nanowires, achieving substantially larger lengths. We believe that our method can be employed to tune a variety of processes that are used to grow nanomaterials such as the vapor–liquid–solid method,[31] the hydrothermal method,[32] and metal-assisted electrochemical etching.[33]

■ ASSOCIATED CONTENT

Ⓢ Supporting Information

Experimental methods on the model experiments, comparison between the theory and the model experiment, experimental details about temperature control units, nanowire synthesis, characterization, and estimation of the diffusion variation across the channel under a temperature gradient. This material is available free of charge via the Internet at http://pubs.acs.org/.

■ AUTHOR INFORMATION

Corresponding Authors

*E-mail: hhcho@yonsei.ac.kr.
*E-mail: hastone@princeton.edu.

Author Contributions

§These authors contributed equally to this work.

Notes

The authors declare no competing financial interest.

■ ACKNOWLEDGMENTS

The authors thank I. Rubinstein, S. Sunderasan, and Z. Zheng for valuable comments and discussions. We thank the NSF for supporting H.A.S. under a grant (No. DMS-1219366), and the NRF of Korea and KETEP for supporting H.H.C. under Grant No. 2011-0017673 and No. 20134030200200, respectively. S.S. acknowledges the NRF of Korea for supporting through the Basic Science Research Program (No. 2013R1A6A3A03020179). T.T.A.-H. is supported by the Wallace Memorial Fellowship at Princeton University.

■ REFERENCES

(1) Cui, Y.; Lieber, C. M. *Science* **2001**, *291*, 851–853.
(2) Gudiksen, M. S.; Lauhon, L. J.; Wang, J.; Smith, D. C.; Lieber, C. M. *Nature* **2002**, *415*, 617–620.
(3) Duan, X.; Fu, T.-M.; Liu, J.; Lieber, C. M. *Nano Today* **2013**, *8*, 351–373.
(4) Hochbaum, A. I.; Chen, R.; Delgado, R. D.; Liang, W.; Garnett, E. C.; Najarian, M.; Majumdar, A.; Yang, P. *Nature* **2008**, *451*, 163–168.
(5) Chan, C. K.; Peng, H.; Liu, G.; McIlwrath, K.; Zhang, X. F.; Huggins, R. A.; Cui, Y. *Nat. Nanotechnol.* **2008**, *3*, 31–35.
(6) Xu, S.; Qin, Y.; Xu, C.; Wei, Y.; Yang, R.; Wang, Z. L. *Nat. Nanotechnol.* **2010**, *5*, 366–373.
(7) Cao, G.; Liu, D. *Adv. Colloid Interface Sci.* **2008**, *136*, 45–64.
(8) Martin-Gonzalez, M.; Snyder, G. J.; Prieto, A. L.; Gronsky, R.; Sands, T.; Stacy, A. M. *Nano Lett.* **2003**, *3*, 973–977.
(9) Abramson, A. R.; Kim, W. C.; Huxtable, S. T.; Yan, H.; Wu, Y.; Majumdar, A.; Tien, C.-L.; Yang, P. *J. Microelectromech. Syst.* **2004**, *13*, 505–513.
(10) Trahey, L.; Becker, C. R.; Stacy, A. M. *Nano Lett.* **2007**, *7*, 2535–2539.
(11) Keyani, J.; Stacy, A. M.; Sharp, J. *Appl. Phys. Lett.* **2006**, *89*, 233106.
(12) Shin, S.; Cho, H. H. *Electrochim. Acta* **2014**, *117*, 120–126.
(13) Schönenberger, C.; van der Zande, B. M. I.; Fokkink, L. G. J.; Henny, M.; Schmid, C.; Kruger, M.; Bachtold, A.; Huber, R.; Birk, H.; Staufer, U. *J. Phys. Chem. B* **1997**, *101*, 5497–5505.
(14) Yin, A. J.; Li, J.; Jian, W.; Bennett, A. J.; Xu, J. M. *Appl. Phys. Lett.* **2001**, *79*, 1039.
(15) Sauer, G.; Brehm, G.; Schneider, S.; Nielsch, K.; Wehrspohn, R. B.; Choi, J.; Hofmeister, H.; Gösele, U. *J. Appl. Phys.* **2002**, *91*, 3243–3247.
(16) Lee, J.; Farhangfar, S.; Lee, J.; Cagnon, L.; Scholz, R.; Gösele, U.; Nielsch, K. *Nanotechnology* **2008**, *19*, 365701.
(17) Shin, S.; Kong, B. H.; Kim, B. S.; Kim, K. M.; Cho, H. K.; Cho, H. H. *Nanoscale Res. Lett.* **2011**, *6*, 467.

(18) Taberna, P. L.; Mitra, S.; Poizot, P.; Simon, P.; Tarascon, J.-M. *Nat. Mater.* **2006**, *5*, 567−573.
(19) Shin, S.; Kim, B. S.; Kim, K. M.; Kong, B. H.; Cho, H. K.; Cho, H. H. *J. Mater. Chem.* **2011**, *21*, 17967−17971.
(20) Schlörb, H.; Haehnel, V.; Khatri, M. S.; Srivastav, A.; Kumar, A.; Schultz, L.; Fähler, S. *Phys. Status Solidi B* **2010**, *247*, 2364−2379.
(21) Grujicic, D.; Pesic, B. *Electrochim. Acta* **2002**, *47*, 2901−2912.
(22) Hahn, D. W.; Özişik, M. N. *Heat Conduction*, 3rd ed.; Wiley: Hoboken, NJ, 2012.
(23) Tikhonov, A. N.; Samarskii, A. A. *Equations of Mathematical Physics*, 3rd ed.; Pergamon Press: Oxford, England, 1963.
(24) Bird, R. B.; Stewart, W. E.; Lightfoot, E. N. *Transport Phenomena*; John Wiley & Sons: New York, NY, 2007.
(25) The remaining conditions are $c(0,t) = c_0$ and $c(\delta(t),t) = 0$. The latter boundary condition assumes that the electrochemical reaction at the solid−liquid interface is much faster than the diffusion of ions.
(26) For $\beta \ll 1$, equation 4 can be written as $2\beta^2 = M_W c_0/A\rho + O(\beta^4)$.
(27) Al-Housseiny, T. T.; Tsai, P. A.; Stone, H. A. *Nat. Phys.* **2012**, *8*, 747−750.
(28) Al-Housseiny, T. T.; Stone, H. A. *Phys. Fluids* **2013**, *25*, 092102.
(29) Al-Housseiny, T. T.; Christov, I. C.; Stone, H. A. *Phys. Rev. Lett.* **2013**, *111*, 034502.
(30) Sun, X.; Zhang, Z.; Dresselhaus, M. S. *Appl. Phys. Lett.* **1999**, *74*, 4005−4007.
(31) Wagner, R. S.; Ellis, W. C. *Appl. Phys. Lett.* **1964**, *4*, 89−90.
(32) Liu, B.; Zeng, H. C. *J. Am. Chem. Soc.* **2003**, *125*, 4430−4431.
(33) Peng, K.; Wu, Y.; Fang, H.; Zhong, X.; Xu, Y.; Zhu, J. *Angew. Chem., Int. Ed.* **2005**, *44*, 2737−2742.